# Tapered Transmission Lines With Dissipative Junctions

Paul D. Dresselhaus, Michael M. Elsbury, *Student Member, IEEE*, and Samuel P. Benz, *Senior Member, IEEE*

***Abstract*—NIST is optimizing the design of a 10 V programmable Josephson voltage standard so that it uses less microwave power by employing fewer parallel-biased arrays with higher voltage per array. Increasing the voltage per array by adding more junctions is challenging because the dissipation of the over-damped Josephson junctions limits the total number that may be located in each array. If there is too much dissipation in the array, the junctions at the end receive too little microwave power compared with the junctions at the beginning of the array. To compensate for the junction attenuation, tapered impedance transmission lines were used to maintain a nearly constant microwave current along the lossy transmission line. Simulation and testing have improved the microwave uniformity of our designs for tapered impedances from 85 Ohms to 5 Ohms. Low-leakage bias tees for various characteristic impedances were designed so that sub-arrays could be measured within long arrays. These tapered arrays have improved the bias current margins, junction number, and bandwidth of NIST junction arrays.**

**By measuring the microwave power from the output of these long arrays, harmonic generation and the nonlinear properties of dissipative junction arrays are studied.**

***Index Terms*—Josephson arrays, nonlinear circuits, superconducting transmission lines, superconductor-normal-superconductor devices.**

## I. Introduction

THE Josephson effect has enabled a broad range of voltage standard applications because a Josephson junction can act as a perfect frequency to voltage converter [1]–[4]. The challenge has always been to produce practical voltages by making arrays with sufficiently large numbers of junctions, driven at sufficiently high frequencies. Typically, a 10 V programmable Josephson voltage standard (PJVS) driven at 16 GHz requires over 300,000 junctions [5].

Long arrays of microwave-biased JJs form the basis for all Josephson voltage standards (JVS). The maximum number of series-connected junctions in an array is limited by the microwave drive uniformity, because a sufficiently uniform excitation is needed to ensure that all the junctions are biased on a constant-voltage step. One of the main challenges for voltage standards is to increase the number of junctions per array, and thus the voltage across the array. In order to improve the microwave uniformity, dc JVS systems, including PJVS and conventional JVS, have microwave biased a number of arrays in parallel by using microwave splitters [2]–[4]. However, applications that exploit pulse-driven biasing, such as ac Josephson voltage standards (ACJVS), for which the broadband bias cannot be simply divided with a fixed-frequency splitter, require separate microwave drives for each array [4]. In all of these applications, the utility of longer arrays is clear: resultant higher voltages and lower input microwave power, which is a limiting factor in some applications.

In general for a JVS, more junctions in an array will produce a higher voltage for a fixed microwave frequency. Traditionally, the attenuation of superconductor-normal metal-superconductor (SNS) arrays has limited the number of junctions per array to $N < Z_0/R_n$, where $Z_0$ is the transmission line impedance and $R_n$ is the junction normal resistance [6], [7]. Arrays that use junctions with insulating barriers, such as superconductor-insulator-superconductor (SIS) and superconductor-insulator-normal-metal-insulator-superconductor (SINIS), can extend this number because the junction capacitance shunts the microwave current, resulting in less attenuation than for SNS junctions. SINIS junctions also are believed to be somewhat self-driven [8], [9], further augmenting the maximal number. For SNS junctions, microwave energy is dissipated and self-generation is not expected to be large. Thus, in order to have large number of SNS junctions in a single array, the array must be designed so that the junctions at the end of the transmission line have constant-voltage steps extending over nearly the same current bias range as the junctions at the beginning, even though they have less microwave power applied.

In this work, tapered transmission lines with decreasing impedance are used [10] to compensate for the decreasing power along the array [11]. Another possible technique to compensate for the reduced power in long arrays would be to reduce the junction size; however this leads to higher-resistance junctions, which have yet higher dissipation toward the end of the array. Since a Josephson junction is driven by current, the microwave power may be transformed to maintain a constant current by using the impedance of the transmission line. Lowering the transmission line impedance increases current and reduces voltage for a given power. This causes negligible reflection as long as the impedance change occurs over a distance on the order of the wavelength of the microwave excitation. The use of arrays in tapered transmission lines has already enabled 275 mV (rms) ACJVS circuits [12], [13] and will be a key technique in the design of the NIST 10 V turnkey PJVS system [14].

Manuscript received August 26, 2008. Current version published July 10, 2009.

P. D. Dresselhaus and S. P. Benz are with the National Institute of Standards and Technology (NIST), Boulder, CO 80305, USA (e-mail: paul.dresselhaus@nist.gov; benz@boulder.nist.gov).

M. M. Elsbury is with the Department of Electrical and Computer Engineering, University of Colorado at Boulder, Boulder, CO 80309-0425, USA (e-mail: mike.elsbury@nist.gov).

Color versions of one or more of the figures in this paper are available online at http://ieeexplore.ieee.org.

Digital Object Identifier 10.1109/TASC.2009.2019245

1051-8223/$25.00 © 2009 IEEE

In addition to attenuation of the microwave power, there are also nonlinear processes that generate higher-order harmonics of the drive frequency. Measurements of these nonlinearities are also presented in this paper.

## II. Fabrication

Circuits were made using the typical NIST voltage standard process for fabrication of SNS junctions with amorphous $\mathrm{Nb_xSi_{1-x}}$ barriers [15]. A three-junction stack is created by depositing an initial Nb base electrode of 350 nm approximate thickness, followed by three alternating 32 nm thick $\mathrm{Nb_{0.08}Si_{0.92}}$ barriers and two 70 nm thick Nb middle electrodes, all of which is capped with a 195 nm thick Nb counter electrode. Once the junction stack is patterned, the base electrode is patterned, followed by deposition and patterning of an 350 nm thick $\mathrm{SiO_2}$ insulator layer and 600 nm thick Nb wiring layer and 120 nm thick AuPd resistor layer. Finally, a 280 nm thick passivation oxide is deposited and patterned and 250 nm thick PdAu pads are deposited and lifted off.

## III. Microwave Design and Measurements

### A. Linear Behavior

Constant-impedance transmission lines (not tapered) have traditionally been used to transmit the microwave energy along arrays. Because the transmission lines themselves are superconducting, the energy loss attributed to the lines themselves is negligible. However, loading the transmission line with junctions inserts a loss mechanism so that the power loss per junction is approximately $\gamma P_i R_n/Z_0$, where $P_i$ is the incident power, $R_n$ is the normal-state resistance of the junction, $Z_0$ is the characteristic impedance of the transmission line, and $\gamma$ is a factor less than unity that depends on how much of the microwave current is dissipated in the barrier. In general, $\gamma$ is a complex function of microwave frequency, dc and microwave bias current, and the characteristic frequency of the junction, $f_c = I_c R_n \mathrm{K_{J-90}}$, where $I_c$ is the critical current and $\mathrm{K_{J-90}}$ is the Josephson constant ($\mathrm{K_{J-90}} = 0.4835979\ \mathrm{GHz}/\mu\mathrm{V}$). To achieve total array power loss less than a few decibels, the number of junctions in the array is limited to $\mathrm{N} \leq \mathrm{Z/Rn}$, which, for 50 $\Omega$ impedance and 5 $\mathrm{m}\Omega$ junctions, is less than 10,000 junctions.

Tapering the impedance of the transmission line compensates for the junction attenuation by transforming the forward-going microwave power along the array to maintain a constant microwave current. In a simplified circuit model, if junction $n$, modeled as a series resistance $\mathrm{R_n} \ll \mathrm{Z(n)}$, dissipates a fraction $\mathrm{R_n}/\mathrm{Z}(n)$ of the power, then a power, $\mathrm{P(n+1)} = \mathrm{P(n)}(1 - \mathrm{R_n}/\mathrm{Z}(n))$ is delivered to the $n+1^{th}$ junction. With the impedance at the next junction set to $\mathrm{Z}(n+1) = \mathrm{Z}(n)(1 - \mathrm{R_n}/(\mathrm{Z}(n)))$, the microwave current, $\mathrm{I(n)} = \sqrt{\mathrm{P(n)/Z(n)}}$, stays constant. In practice, this is done in a continuous manner such that the coplanar waveguide (CPW) gap of the transmission line is smoothly varied on a length scale on the order of the microwave wavelength. Clearly, the impedance may not be reduced indefinitely, as the power will eventually decay to zero, but, in theory, tapering increases the number of junctions in an array receiving a nearly constant microwave current. Another advantage of tapering the transmission line is that the increased number of junctions utilizes a larger fraction of the microwave power, leaving less power to be dissipated in the termination resistor. This minimization of the power wasted in the termination resistors is important for optimizing the 10 V PJVS system design for minimal microwave input power and minimal heat load of the circuit at 4 K.

In order to test the microwave power distribution in arrays embedded in tapered transmission lines, a series of test chips was designed in which a long array was subdivided into many series-connected subarrays that could be independently measured. Current-voltage curves (IVCs) are shown in Fig. 1 for subarrays of identical junction number at both the beginning and near the end of either tapered (b) or non-tapered (a) transmission lines with a 15 GHz signal applied with similar powers.

In order to understand the role of microwaves on the IVC, it is convenient to keep track of three points on the IVC: the maximum current $\mathrm{I_0}$ of the zero-voltage step, and the minimum $\mathrm{I_1}$ and maximum $\mathrm{I_2}$ current at which the array is on the first non-zero constant-voltage step. These points are indicated by the arrows in Fig. 1(b). Typically, the arrays are operated at a microwave power and frequency such that the zero-voltage steps have larger current-ranges than the first step. Under this condition, $\mathrm{I_0}$ and $\mathrm{I_2}$ generally both track the junction with the most power driving it off the constant-voltage step, while $\mathrm{I_1}$ tracks the last junction that receives just enough power so that it is on the step. Typically $\mathrm{I_2}$ tracks $\mathrm{I_0}$ if the junction uniformity is good enough (which is borne out in the dc IVCs). However, the nonlinearity of the array will change the dissipation between the zero-voltage and first steps, leading to variations in these measured values.

In general, the dc and microwave currents will be applied from the top to the bottom of the array, but the voltage may be measured at any sub-array. To achieve the most number of junctions in an array, the impedance should be tapered from the highest to the lowest practical values. In order to maximize the starting impedance, the longest arrays (15,600 junctions) used a 50 $\Omega$ to 86 $\Omega$ broadband impedance transformer made from lumped-element quarter-wave sections [16]. The largest impedance readily available was chosen to be 86 $\Omega$ from simulations using Ansoft's HFSS [17] with a coplanar waveguide (CPW) with 225 $\mu$m total width, having 60 $\mu$m gaps and 16 $\mu$m center-conductor width. Bias tees were designed and simulated to verify microwave operation with less than −20 dB reflection in the 10 GHz to 25 GHz band of interest. In addition to minimal reflection, the bias tee must also isolate the dc port from microwave power; this is accomplished by the use of inductive planar spirals operating below their resonance frequency. The use of many bias tees on a long array allowed measurement of the voltage steps in each subarray, so that the microwave attenuation could be inferred from the power dependence of each subarray.

High-impedance CPW sections were designed by enlarging the gap: a typical 50 $\Omega$ CPW in this technology had a 6 $\mu$m gap whereas an 86 $\Omega$ had a 60 $\mu$m gap. By reducing the CPW gap to 2 $\mu$m, the impedance could be scaled down to 32 Ohms.

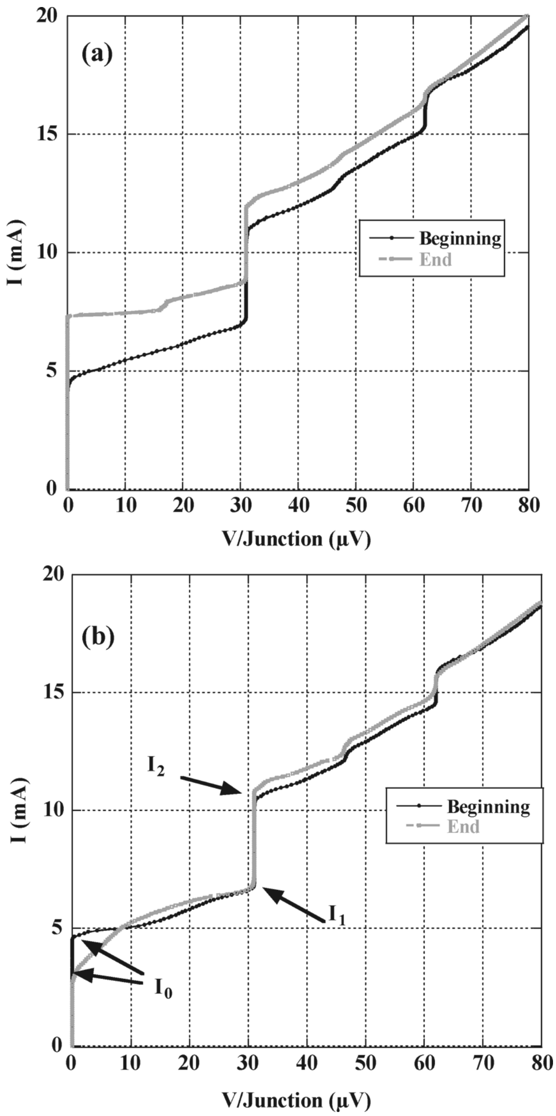


Fig. 1. Current-voltage curves (IVC) for two sets of subarrays from (a) non-tapered and (b) a tapered transmission lines. For the non-tapered lines, the current ranges of the constant voltage steps suggest that the end array clearly receives less microwave power than the beginning array. The subarrays of the tapered line (b) show nearly overlapping steps, indicating similar microwave current. Both chips had similar junction parameters of $I_c = 8.5$ mA and $R_n = 4.8$ mΩ. All measurements were taken at a temperature of 4 K.

To further reduce the impedance, the gap was further decreased by increasing the base electrode layer width, bringing it closer to, and eventually underneath, the wiring layer to form a waveguide structure that is a hybrid of microstrip and coplanar waveguide. Unfortunately for this taper approach, there is a transition region between the CPW and hybrid regime in which the impedance is extremely sensitive to the lithographic tolerance of the wiring and base electrode layers. In order to reduce the effects of lithography, small tabs were patterned into the base electrode such that the specific capacitance of a cell was determined mostly by the area of the tab, rather than the patterned separation of wiring and base electrodes, as shown in Fig. 2. In this regime, the impedance was tapered by increasing the length of this overlapping tab, rather than changing the overlap width. This was found to increase the yield of the tapering process. By use of HFSS to simulate the structures, these techniques allowed the waveguide impedance to continuously change from 86 Ω to 5 Ω.

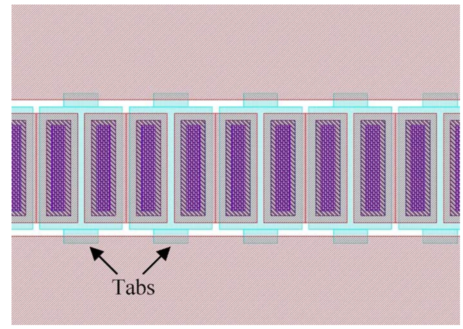


Fig. 2. Transition segment from CPW to hybrid waveguide with base electrode tabs. In the pure CPW section, there is no overlap between the center conductor and the outer return path. For the hybrid CPW/microstrip transmission line, the base electrode overlaps the wiring.

In addition to the subdivided array, there is another array on the chip with identical tapering, but having microwave ground ties (tying the two sides of the CPW ground together) instead of bias tees. The bias tees at the top and bottom of this array remain in order to bias the array. By comparing these structures, the residual parasitic leakage and reflections of the bias tees were inferred.

It is important to note that, because junction dissipation is a function of dc bias, the transmission line attenuation will also, in general, be a function of dc current bias as well as frequency. Attenuation is minimized when the junctions are biased near zero dc current, where the dissipation is governed by the fraction of the current through the quasi-particle channel. The dissipation while biased on the first step is more complicated, but the relevant resistance may be approximated to first order as $R_n$, the normal-state resistance of the junction. This bias-dependant attenuation leads to the choice of tapering the array to optimize either the zero-voltage or first steps. Because nonuniformities will reduce the current range of the first step far more than that of the zero-voltage step, a "taper factor" of 5/6 was chosen (somewhat arbitrarily) to skew the optimization slightly toward the first step. Run-to-run variations in the targeting of $R_n$ also skew the optimization proportionally.

Fig. 3 shows the cell dependence of the current range of the first step (defined as $I_2 - I_1$), and Fig. 4 shows the cell-dependence of the current-range of the zero-voltage step ($\mathrm{I}_0$) for an array with 15 GHz microwave drive, $I_c = 6.9$ mA, $R_n = 6.2$ mΩ, and the transmission line is tapered from 86 to 18.5 Ω. For all of these measurements, the current range for a step is defined as the current for which the voltage is within 10 $\mu$V of the absolute step voltage. The array is divided into 20 subarrays with 828 junctions each, with subarray #1 closest to the microwave launch and impedance transformer and subarray #20 closest to the termination resistor. The maximum current range of the first step moves to higher applied powers for subarrays closest to the termination, while the zero-voltage step current ranges have much slower dependence on tap location.

The current range of the last cell (#20) in Fig. 3 appears to require more power (a few decibels) compared to most of the

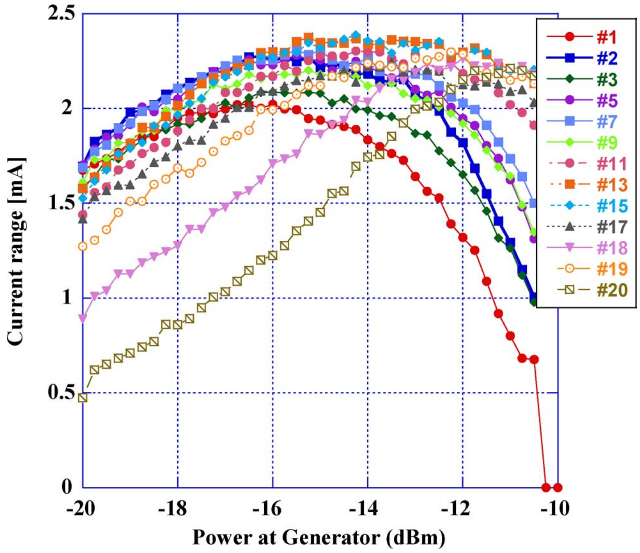


Fig. 3. Current range $(I_2 - I_1)$ of the first constant voltage step for a collection of subarrays within a 15,600 junction array. Data from several inner subarrays are omitted for clarity. The subarray number increases for arrays furthest from the microwave source.

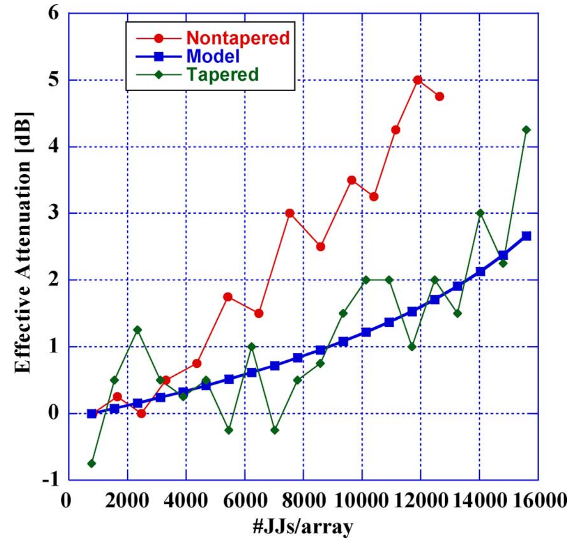


Fig. 5. Inferred attenuation along tapered and nontapered transmission lines loaded with junction arrays driven at 15 GHz. The model takes into account the designed tapering factor. Note that the nontapered array has only 12,648 junctions, because this is the longest array in which a constant-voltage step could be obtained.

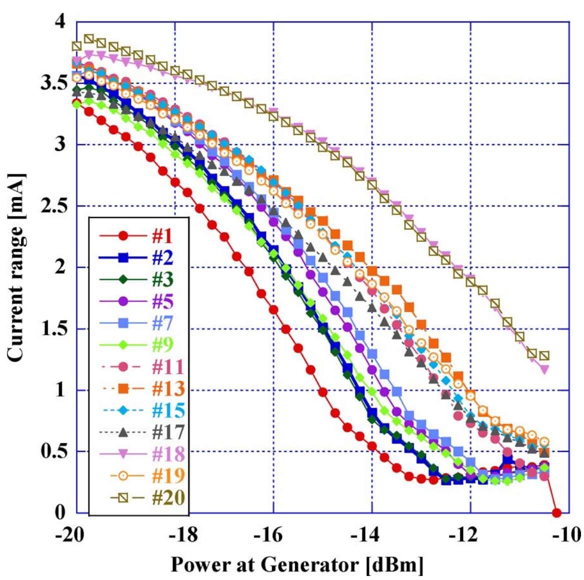


Fig. 4. Current range $(I_0)$ of the zero-voltage step as a function of power at the generator for the same collection of subarrays as in Fig. 3. The last few cells behave in an non-monotonic manner.

other subarrays (although subarray #18 is also shifted somewhat), indicating that there is some power reduction in the last array. The first subarray (#1) also shows a slightly smaller step. This behavior is typical of our tapered arrays, and a complete explanation remains unclear, although varying the value of the termination resistor had little effect on these phenomena. The array without bias tees on this same die (not shown) had a first step with larger current range at most frequencies. This suggests that these phenomena may be caused partially by reflections or losses from the bias tees.

Nonetheless, there are large ranges in both microwave bias power and dc bias current over which the constant-voltage steps shown in Figs. 3 and 4 are quantized for all 15,600 junctions in the array. This was not possible without tapering the transmission line impedance.

Fig. 5 shows the effective attenuation of the junction array. This is defined as the power at which there is a maximum of the first step's current range. Power is normalized to the power required to maximize the first step for the first subarray. The model assumes that a fraction, $Rn/Z$, of the power is dissipated in each junction.

Fig. 6 shows the current range of the first constant-voltage step in a range of frequencies between 10 GHz and 25 GHz. The current step decreases nearly monotonically and disappears above ~22 GHz in all but the first few subarrays. The problems at high frequency, namely zero current range or relative minima, are caused most likely by a combination of junction nonuniformity and power nonuniformity (or loss) caused by the microwave bias tees. Because optimizing the power did not significantly improve the results for this figure, the power is held constant over the entire frequency range.

Because microwave reflections in this circuit may cause standing waves, it is important to model and optimize the microwave performance as well as the dc junction uniformity. For this purpose, HFSS is used to simulate and optimize all of the critical elements. These include the bias tees, the transmission line impedance, the impedance transformer on the feed, the corners in the transmission line, and the termination resistors. Because the circuit is too complex to enter into a finite-element simulator in its entirety, it is assumed that splitting the circuit into elements and optimizing each element, then performing a circuit simulation using the cascaded port responses of the elements, is sufficient. This assumption will break down if elements are strongly coupled via mechanisms not modeled by the CPW port, e.g., radiation.

A comparison of a nontapered array of 12,648 junctions and a tapered array of 15,600 junctions is shown in Fig. 7. The voltage per junction with a 15 GHz microwave drive is plotted vs. bias

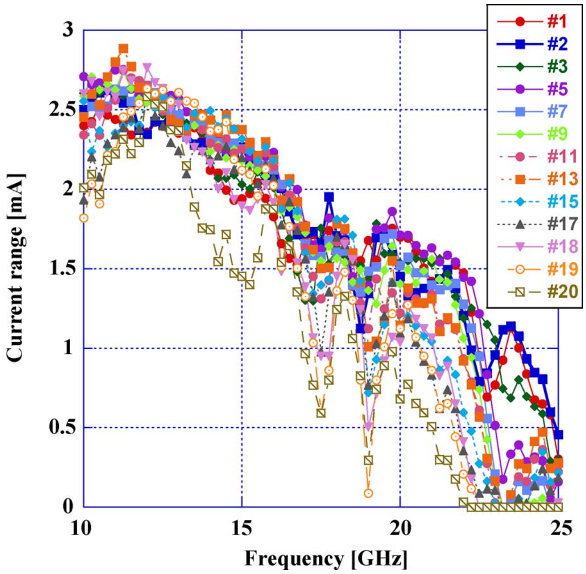


Fig. 6. The frequency dependence of the first constant-voltage step for various subarrays of the device shown in Figs. 3 and 4.

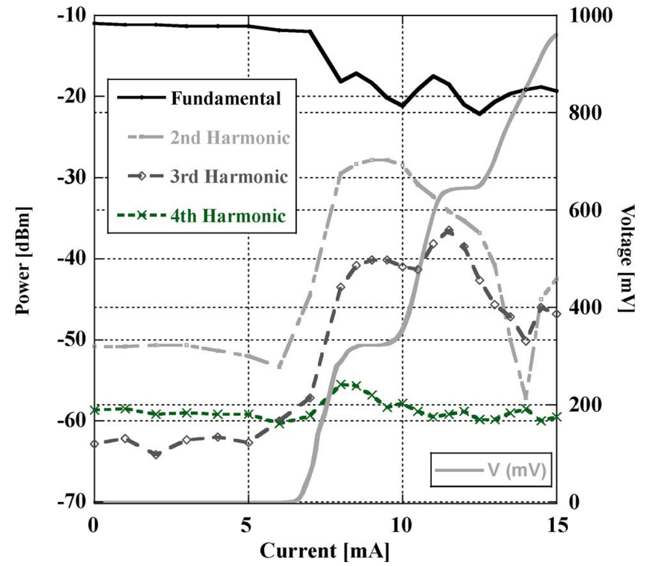


Fig. 8. Observed nonlinearities at the output of a long (15,600 junction) array. The right axis corresponds to the IVC shown as a solid grey line.

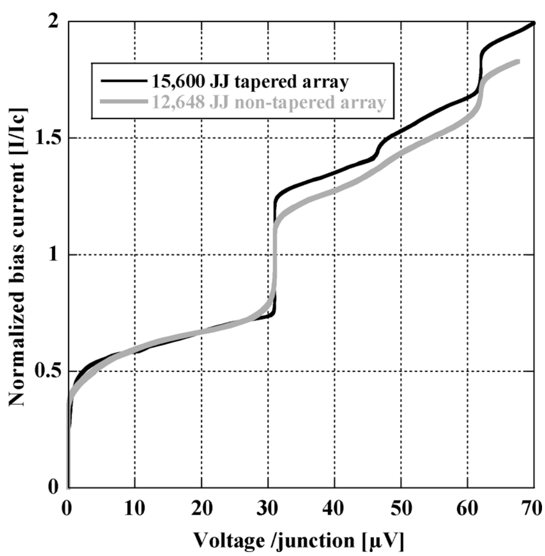


Fig. 7. Comparison of IVCs of complete arrays in both tapered and nontapered transmission lines. For nontapered lines, the shorter, 12,648 junction array is shown, while the array in the tapered line contains 15,600 junctions. The amplitude of the 15 GHz microwave power was tuned in each case to maximize the current range of the first step.

current. Even though there are more junctions (the junction parameters are similar) in the tapered array, the constant-voltage step is larger and the transitions are sharper, indicating better microwave uniformity. Clearly the tapered array has a larger step range.

## *B. Non-Linear Behavior*

In order to better understand the nonlinear behavior of these long arrays of Josephson junctions, another test circuit was designed that is similar to the circuit described above, except that the termination resistor was replaced with a 10 dB attenuator matched to the termination impedance. Thus 90% of the incident microwave energy is absorbed in the attenuator, ensuring a good match, and 10% is transmitted off the chip via an output microwave launch. The spectrum of the output waveform was measured with a spectrum analyser to display and extract the harmonic and subharmonic signals. The bandwidth of the cabling and microwave launch limited measurements to below ~40 GHz. In addition, the high-frequency (greater than 15 GHz) attenuation of the probe made quantitative analysis of the data difficult [18].

Fig. 8 shows the magnitude of the fundamental, second, third and fourth harmonics that were measured when the array was driven at 10 GHz. The corresponding voltage of the IVC is plotted on the right axis. The low, 10 GHz, frequency was chosen so that the largest number of harmonics would be observable in the output bandwidth of the measurement probe. Signals above 20 GHz were strongly attenuated, and no signals above 45 GHz were observed.

When biased in the zero-voltage state, the array has little harmonic generation. As the bias approaches the first step, both the second, third, and fourth harmonics rise. The third harmonic rises even more on the $n = 2$ constant voltage step. The power of the fundamental also reaches relative minima on the $n = 1$ and $n = 2$ constant-voltage steps. Although the frequency-dependent attenuation of the probe and the array leads is not well understood, Fig. 8 clearly shows that the second harmonic is becoming an important part of the waveform on the first constant-voltage step.

These results suggest that harmonic generation is a possible contributing factor to the reduced operating margins (current range) of the last few subarrays in Fig. 3. The bias tees are designed to work in the band of the fundamental, not that of the harmonics. If there is significant harmonic generation, reflections from the bias tee could lead to microwave power nonuniformity in these segments. The use of an absorptive low-pass filter in series with the array could attenuate these higher harmonics, possibly leading to better microwave uniformity in the entire array, and thus larger total constant-voltage steps.

## IV. Conclusion

The use of tapered-impedance transmission lines loaded with Josephson junctions has been shown to extend the number of junctions that may be driven in a single array. For a given critical current, tapering also allows a larger current margin for a given number of junctions in an array. Finally, the increase in the number of junctions from tapering minimizes the power dissipated in the termination resistor. Using these long, dissipative arrays, the output waveform has been measured and shows large harmonic content, particularly when biased on a constant-voltage step, and the results suggest that further improvements in step uniformity are possible.

## Acknowledgment

The authors thank Prof. Zoya Popović for helpful support, Charles J. Burroughs and Alain Rüfenacht for measurement expertise, and David Olaya, Burm Baek, and Norman Bergren for fabrication assistance.

## References

[1] S. Shapiro, "Josephson currents in superconducting tunneling, the effect of microwaves and other observations," *Phys. Rev. Lett.*, vol. 11, pp. 80–82, 1963.

[2] J. Niemeyer, "Josephson voltage standards," in *Handbook of Applied Superconductivity*, B. Seeber, Ed. Philadelphia, PA: Inst. Of Physics Publishing, 1998, vol. 2, p. 1813.

[3] C. A. Hamilton, "Josephson voltage standards," *Rev. Sci. Instrum.*, vol. 71, pp. 3611–3623, Oct. 2000.

[4] S. P. Benz and C. A. Hamilton, "Application of the Josephson effect to voltage metrology," *Proc. of the IEEE*, vol. 92, no. 10, pp. 1617–1629, Oct. 2004.

[5] H. Yamamori, M. Ishizaki, A. Shoji, P. D. Dresselhaus, and S. P. Benz, "10 V programmable Josephson voltage standard circuits using NbN/TiNx/NbN/TiNx/NbN double-junction stacks," *Appl. Phys. Lett.*, vol. 88, p. 042503, Jan. 2006, 3 pages.

[6] R. L. Kautz, "Miniaturization of normal-state and superconducting striplines," *NBS J. Research*, vol. 84, pp. 247–259, May 1979.

[7] R. L. Kautz, "Picosecond pulses on superconducting striplines," *J. Appl. Phys.*, vol. 49, pp. 308–314, Jan. 1978.

[8] K.-T. Kim, M.-S. Kim, and Y. Chong, "Simulations of collective synchronization in Josephson junction arrays," *Appl. Phys. Lett.*, vol. 89, p. 062501, 2006.

[9] J. Hassel, L. Grönberg, P. Helistö, and H. Seppä, "Self-synchronization in distributed Josephson junction arrays studied using harmonic analysis and power balance," *Appl. Phys. Lett.*, vol. 89, p. 072503, 2006.

[10] D. M. Pozar, *Microwave Engineering*, 2nd ed. Hoboken, NJ: Wiley, 1998, pp. 290–292.

[11] P. D. Dresselhaus, S. P. Benz, C. J. Burroughs, N. F. Bergren, and Y. Chong, "Design of SNS Josephson arrays for high voltage applications," *IEEE Trans. Appl. Supercond.*, vol. 17, no. 2, pp. 173–176, June 2007.

[12] S. P. Benz, P. D. Dresselhaus, C. J. Burroughs, and N. F. Bergren, "Precision measurements using a 300 mV Josephson arbitrary waveform synthesizer," *IEEE Trans. Appl. Supercond.*, vol. 17, no. 2, pp. 864–869, June 2007.

[13] S. P. Benz, P. D. Dresselhaus, N. F. Bergren, and R. P. Landim, "Progress toward a 1 V pulse-driven ac Josephson voltage standard," in *2008 Conference on Precision Electromagnetic Measurements Digest*, Broomfield, CO, June 9–13, 2008, pp. 48–49, presented.

[14] P. D. Dresselhaus, M. Elsbury, C. J. Burroughs, D. Olaya, S. P. Benz, N. F. Bergren, R. Schwall, and Z. Popovic, "Design of a turn-key 10 V programmable Josephson voltage standard system," in *2008 Conference on Precision Electromagnetic Measurements Digest*, Broomfield, CO, June 9–13, 2008, pp. 102–103, presented.

[15] B. Baek, P. D. Dresselhaus, and S. P. Benz, "Co-sputtered Amorphous $Nb_xSi_{1-x}$ barriers for Josephson-junction circuits," *IEEE Trans. Appl. Supercond.*, vol. 16, no. 4, pp. 1966–1970, Dec. 2006.

[16] M. M. Elsbury, P. D. Dresselhaus, N. F. Bergren, C. J. Burroughs, S. P. Benz, and Z. B. Popović, "Broadband integrated power dividers for programmable Josephson voltage standards," *IEEE Trans. Microwave Theory and Techniques*, submitted for publication.

[17] This commercial tool is identified in this paper only in order to adequately specify the experimental procedure. Such identification does not imply recommendation or endorsement by the National Institute of Standards and Technology, nor does it imply that the equipment identified is necessarily the best available for the purpose.

[18] M. M. Elsbury, C. J. Burroughs, P. D. Dresselhaus, Z. B. Popović, and S. P. Benz, Microwave Packaging for Voltage Standard Applications these proceedings.